TOWARDS AUTOMATED PHOTOGRAMMETRIC ASSESSMENT OF TRUNK FLEXIBILITY

H. Vieira Neto* and E. B. Neves**

* Graduate Program in Electrical and Computer Engineering
** Graduate Program in Biomedical Engineering
Federal University of Technology – Paraná, Curitiba
e-mail: hvieir@utfpr.edu.br

Abstract: Trunk flexibility is an important parameter in the assessment of the overall health status of a subject and has been the focus of manual photogrammetric studies. A preliminary study towards automating such photogrammetric assessment using image processing techniques – the Generalised Hough Transform and a gradient-based angle estimation algorithm – is presented in this work. The algorithm shows promising results when compared to previous photogrammetric studies using the same image data.
Keywords: Photogrammetry, Trunk Flexibility, Hough Transform.

Introduction

The assessment of body health status involves several physical aspects, such as strength, balance and flexibility. A reduction in flexibility can lead to functional limitations and lower back pain. Some of the main locations for assessing trunk flexibility are the posterior thigh muscles, which are called ischiotibial muscles [1].

In this sense, the most commonly test used to assess trunk flexibility is the sit and reach test (SRT) because of its simplicity and convenience to conduct in large groups. However, studies suggest that the outcome of the SRT is generic and that it has many intervening factors that result in inaccuracies [1, 2].

With the intention to enhance the assessment of trunk flexibility, Perin and colleagues [1] developed an assessment protocol using photogrammetry, a resource that is already successfully used in many protocols in the biomedical field for the assessment of lung volume [3, 4] and the assessment of postural spine deviations in athletes [5] and subjects in general [6].

Photogrammetry is the combination of digital photography and imaging software for the measurement of distances and angles. Although generic image manipulation software can be used for this purpose, there is also software that is specifically designed for postural assessments – an example is SAPO (*Software para Avaliação Postural*, in Portuguese, or Postural Assessment Software), which already has pre-established anatomical landmarks to be identified in the image [7].

However, both in conventional protocols using generic software and other protocols using specific software such as SAPO, there are inaccuracies in tracing lines and angles or in the identification of anatomical landmarks, which depend on the human operator. This problem has been formally investigated before and the conclusion was that inter-operator reliability is low – the method is considered reliable only when a single operator is involved [8, 9].

Regarding the specific case of trunk flexibility, another aspect to be considered is the time for completion of the assessment. The SRT (having the disadvantages already mentioned) is a quick test, but the protocol developed by Perin and colleagues [1] requires the manual measurement of three angles by the operator, which is time consuming and increases the probability of inaccurate measurements.

In this sense, the objective of the present study is to develop software that automatically measures the angles proposed by Perin and colleagues [1] for trunk flexibility assessment using digital image processing techniques, with the objective of improving inter-operator reliability and time spent in the analysis.

Materials and methods

Perin's protocol uses three commercial right-angled polystyrene electrical conduits as markers (Figure 1). These markers are adhered to the surface of the skin on the dorsal region of the subject's trunk, in such a way that they are easily identified in a digital photograph. The markers are placed using double faced adhesive tape in the following anatomical points: fifth lumbar vertebra, twelfth thoracic vertebra and seventh cervical vertebra (Figure 2).

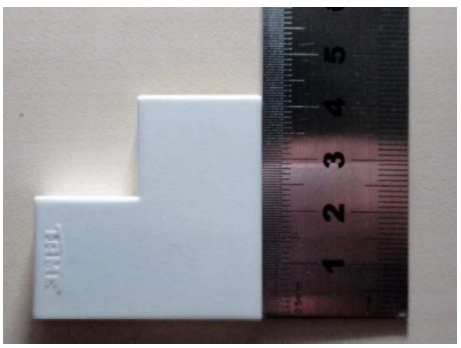

Figure 1: Right-angled polystyrene electrical conduit used as marker [1].

Figure 2: Markers placed on the spine: fifth lumbar vertebra, twelfth thoracic vertebra and seventh cervical vertebra [1].

The protocol follows the same movement used in the sit and reach test, with the subject's feet resting on a standard Wells' bench (31 cm in height, 64.5 cm in length and 40 cm in width) – the test is used to assess the stretching of the posterior region of the trunk and ischiotibial muscles (hamstrings), as shown in Figure 3.

Figure 3: Sit and reach test using a standard Wells' bench in order to measure angles for the assessment of trunk flexibility [1].

Figure 3 also shows five angles used for assessment of trunk flexibility in Perin's protocol (*Fq*, *Fql* and *Fqlt* are measured angles, whereas *Fl* and *Ft* are calculated angles, see Table 1). The intention is to estimate the contribution of different segments of the spine at the end of the trunk flexion movement when performing the sit and reach test.

Table 1: Perin's protocol angles for the assessment of trunk flexibility.

Angle	Measurement / Computation
Fqlt	Lumbar hip thoracic flexion: angle between the upper edge of the marker at the seventh cervical vertebra and a horizontal reference line
Fql	Lumbar hip flexion: angle between the upper edge of the marker at the twelfth thoracic vertebra and a horizontal reference line
Fq	Hip flexion: angle between the upper edge of the marker at the fifth lumbar vertebra and a horizontal reference line
Fl	Lumbar flexion angle: *Fl = Fql – Fq*
Ft	Thoracic flexion angle: *Ft = Fqlt - Fql*

In order to measure and calculate the angles listed in Table 1, digital photographs are taken from the subject at a distance of 200 cm, with a 10 megapixel resolution camera held by a tripod 50 cm high from the floor.

The Generalised Hough Transform [10] is used in order to locate the markers in the digital photographs. For that, a synthetic model of the markers (Figure 4) was used to generate the R-table that votes for candidate locations of the markers within the input image.

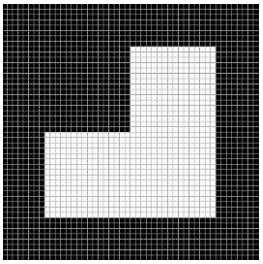

Figure 4: Synthetic model of the markers with the same approximate size (48 × 48 pixels) as the real markers.

The first step in the construction of the R-table [10] is to obtain its centre of mass, by computing the average coordinates of white pixels in the synthetic model. Then, the image gradient is computed using Sobel masks and each edgel (pixel corresponding to a strong edge in the gradient image) is mapped to an entry in the R-table. Each entry in the R-table contains the radius (R) from the coordinates of the edgel (x_i, y_i) to the centre of mass of the model (x_c, y_c), and the relative angle (θ) between the orientation of the local gradient ($\emptyset$) and the direction from the edgel to the centre of mass of the model:

$$R = \sqrt{(x_i - x_c)^2 + (y_i - y_c)^2} \quad (1)$$

$$\theta = \emptyset(x_i, y_i) - \text{atan2}[(y_i - y_c), (x_i - x_c)] \quad (2)$$

The R-table is then used to vote for candidate locations of the markers in the input image, independent of their orientation. This is done by computing the image gradient of the input using Sobel masks and then finding strong edgels (with magnitudes higher than half of the maximum gradient magnitude response). For each strong edgel (x_j, y_j) detected in the gradient of the input image, the R-table is used to increment one vote per entry in each corresponding location in Hough space (a matrix H with the same dimensions of the input image). This is done by computing the direction (α) from the orientation of the local gradient and the relative angles stored in the entries of the R-table, and then voting at locations (x_v, y_v), whose distances are given by the corresponding radii:

$$\alpha = \emptyset(x_j, y_j) - \theta \quad (3)$$

$$x_v = x_j - R\cos\alpha \quad (4)$$

$$y_v = y_j - R\sin\alpha \quad (5)$$

The result at the end of the process is that locations with the highest number of votes in Hough space are likely to correspond to where the markers are located in the input image – as there are three markers, the last step in the transform is to search for the three highest peaks in Hough space.

The final stage of the algorithm concerns measuring the angles of the detected markers with respect to horizontal lines. This is accomplished by first cropping an image patch of 48 × 48 pixels in the surrounding of each detected location and then computing its image gradient. All gradients with orientations above 90º are discarded and the median of the remaining orientations (below 90º) is taken as the approximate measurement of the angle of the marker.

Results and discussion

Experiments were conducted using five input images originally used in the work of Perin and colleagues, which were previously converted to gray levels and had irrelevant regions removed, in order to reduce processing time. An example of input image is given in Figure 5.

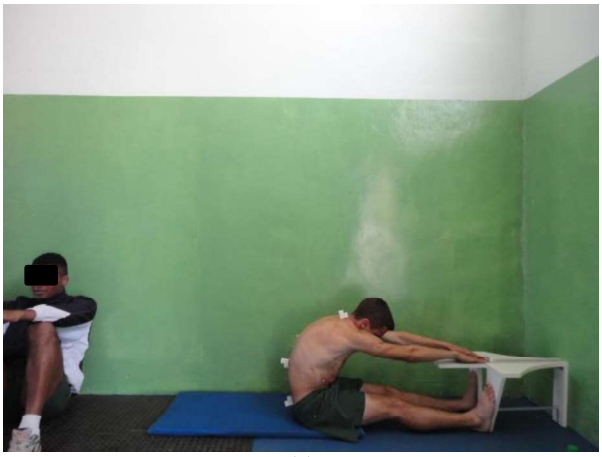

(a)

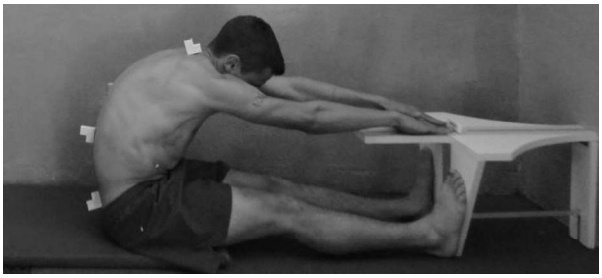

(b)

Figure 5: Photograph from subject 106. (a) Original colour image [1]; (b) Input image converted to gray levels, with regions not corresponding to the subject removed.

Computation of the Generalised Hough Transform in search for the synthetic model of the markers (Figure 4) within the input image corresponding to subject 106 (Figure 5b) resulted in the voting landscape (Hough space) depicted in Figure 6.

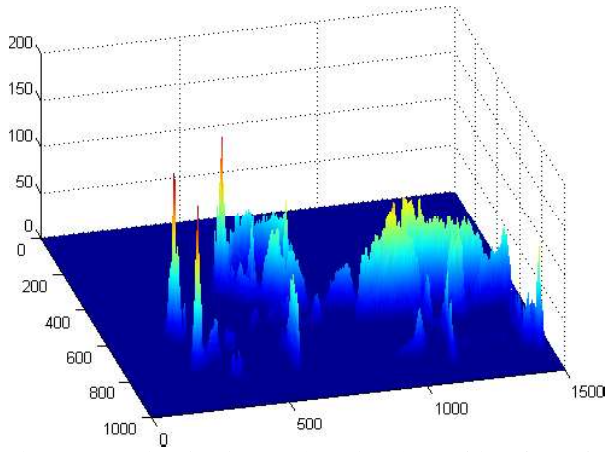

Figure 6: Voting landscape (matrix *H*) resulting from the Generalised Hough Transform in search for the synthetic model of the markers. The three highest peaks correspond to the locations of the markers in the input image of subject 106.

It can be noticed in Figure 6 that the three highest peaks correspond to the locations of the markers in the input image, as shown in Figure 7. The corresponding regions of 48 × 48 pixels were correctly located by the Generalised Hough Transform, independently of the orientation of the markers.

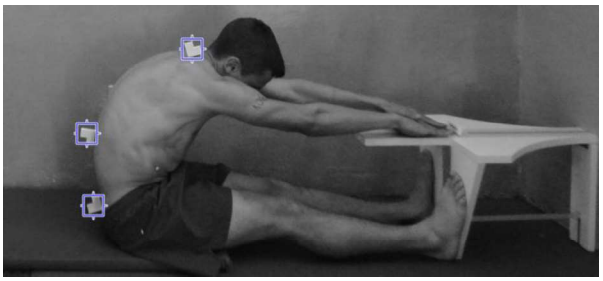

Figure 7: Markers highlighted in the input image of subject 106. The Generalised Hough Transform was able to detect all three markers accurately, regardless of their orientation.

Figure 8 shows the cropped image patches of the markers (48 × 48 pixels) and their rotated versions in order to illustrate the accuracy of the gradient-based procedure used for orientation estimation.

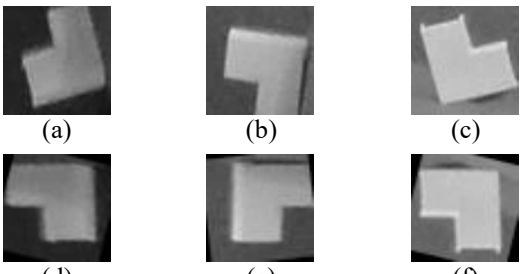

(a) (b) (c)

(d) (e) (f)

Figure 8: Detected markers. (a) *Fq*; (b) *Fql*; (c) *Fqlt*; (d) rotated *Fq*; (e) rotated *Fql*; (f) rotated *Fqlt*. One can notice that the edges of the rotated markers are aligned with the horizontal line.

The results obtained for five subjects (106 to 110) are shown in Table 2, and compared to the ground-truth (manual angle measurements) from the work by Perin and colleagues.

Table 2: Results obtained for measured angles *Fq*, *Fql* and *Fqlt* for subjects 106 to 110 and corresponding ground-truth.

	Ground-truth (deg.)			Autom. Meas. (deg.)		
Sub	*Fq*	*Fql*	*Fqlt*	*Fq*	*Fql*	*Fqlt*
106	79.29	93.50	168.7	76.04	96.46	166.3
107	84.81	111.5	182.9	75.04	111.1	185.9
108	75.38	112.4	165.3	74.55	110.6	193.5
109	105.4	119.1	201.3	106.9	116.6	197.2
110	99.46	120.6	180.0	99.14	119.8	175.0

The errors between automatic and manual angle measurements are given in Table 3, where one can notice that most results are below 5%. Larger errors were obtained for *Fq* for subject 107 and *Fqlt* for subject 108.

Table 3: Error between automatically measured angles and manually measured angles (ground-truth) from the work by Perin and colleagues.

	Error (%)		
Subject	*Fq*	*Fql*	*Fqlt*
106	4,10	-3,17	1,44
107	**11,5**	0,30	-1,65
108	1,10	1,56	**-17,1**
109	-1,36	2,09	2,00
110	0,32	0,63	2,79

A more rigorous analysis revealed that the manual measurement for *Fq* for subject 107 was more accurate than the automatic measurement, but the automatic measurement for *Fqlt* for subject 108 was more accurate than the manual measurement. This analysis shows that marker angles closer to the horizontal reference line are more accurately estimated by the automatic method than marker angles closer to 90º.

Conclusion

This paper presented an automated technique for photogrammetric assessment of trunk flexibility based on Perin's protocol [1], aiming at increasing reliability in the measurement of marker angles. The technique is based on the Hough Transform and a gradient-based angle estimation algorithm.

Preliminary experimental results show that errors are mostly within ±5%, except in cases in which marker angles are close to 90º. A small change in the original protocol, regarding the standardisation of orientations while positioning markers may improve accuracy in marker angle estimation significantly.

Future work will focus on investigating different algorithms for the estimation of angles in order to improve measurement accuracy.

Acknowledgements

The authors thank Andréa Perin for providing the original input images and their respective manual angle measurements.

References

[1] Perin A, Neves EB, Ulbricht L. Protocolo de Avaliação do Nível de Flexibilidade dos Isquiotibiais por Fotogrametria. Revista Brasileira de Inovação Tecnológica em Saúde. 2013; 3(1):1-14.

[2] Perin A, Ulbricht L, Ricieri DdV, Neves EB. Use of Biophotogrammetry for Assessment of Trunk Flexibility. Revista Brasileira de Medicina do Esporte. 2012; 18(3):176-180.

[3] Ripka WL, Ricieri DdV, Ulbricht L, Neves E, Wan Stadnik AM, Romaneli EFR. Biophotogrammetry Model of Respiratory Motion Analysis Applied to Children. In: Proceedings of The 34th Annual International Conference of The IEEE EMBS, 2012. p. 2404-2407.

[4] Ripka WL, Ulbricht L, Neves EB, Gewehr PM. 2D and 3D Photogrammetric Models for Respiratory Analysis in Adolescents. In: Proceedings of the 13th Mediterranean Conference on Medical and Biological Engineering and Computing, 2014. p. 1063-1066.

[5] de Macedo RMB, Ulbricht L, Ricieri DdV, Preis C, Duarte JM, Bertassoni Neto L. Análise Cinemática 2D da Postura Ortostática de Ciclistas Lombálgicos. Revista Uniandrade. 2013; 14(1):07-23.

[6] Vacari DA, Ulbricht L, Schneider FK, Neves E B. Principais Métodos de Diagnóstico Postural da Coluna Lombar. Revista da Educação Física (UEM). 2013; 24(2):305-315.

[7] Souza JA, Pasinato F, Basso D, Corrêa ECR, da Silva AMT. Biophotogrammetry: Reliability of Measurements Obtained with a Posture Assessment Software (SAPO). Revista Brasileira de Cineantropometria e Desempenho Humano, 2011; 13(4):299-305.

[8] Gatto-Cardia MC, de Lucena NMG, Hermoso VMS, Soares LMDMM, de Almeida MÂRP, de Carvalho AGC, Barros MDFA. Estudo de Fiabilidade Inter-examinador na Fixação de Marcadores Anatômicos para Avaliação Postural Fotogramétrica. Revista Brasileira de Ciências da Saúde. 2012; 16(2):51-58.

[9] Carneiro PR, Cardoso BdS, da Cunha CM, Teles LCdS. Confiabilidade Inter e Intraexaminador da Avaliação Postural da Cabeça por Fotogrametria Computadorizada. Fisioterapia e Pesquisa. 2014; 21(1):34-39.

[10] Ballard DH. Generalizing the Hough Transform to Detect Arbitrary Shapes. Pattern Recognition. 1981; 13(2): 111-122.